

The comparison of the gain flattening techniques EDFA configurations in the C/L band

M. YUCEL*, G. YENILMEZ

Department of Electrical-Electronics Engineering, Faculty of Technology, Gazi University, Ankara, Turkey

In this study, conventional band (C band) erbium doped fibre amplifiers (EDFA) and long band (L band) EDFAs are analyzed to obtain better flat gain characteristics. For this purpose, three C band EDFA and two L band EDFA configurations are established. The effects of the fibre Bragg grating (FBG), gain flattening filter (GFF), two stage system, optical feedback loop, and amplified spontaneous emission (ASE) reflection techniques are observed in these configurations. Among all configurations two-stage EDFA with GFF and uniform FBG (UFBG) has the lowest ripple results in C band. In L band, the results of the two-stage EDFA with optical feedback loop are close to other L band structure but have better results.

(Received July 28, 2014; accepted September 9, 2015)

Keywords: ASE reflection, C band EDFA, Gain flattening, FBG, L band EDFA

1. Introduction

Nowadays, EDFAs and WDM systems are the solution in the ultra-long haul fibre optical communication systems. EDFAs are used in S (short) band, C band and L band in consequence of the rapidly increased capacity needs [1, 2]. Many different configurations have been developed to increase the gain of EDFAs in C and L band. In these configurations, single-stage system which is used an erbium doped fibre (EDF) has been pumped in several ways. Then, EDFA that has part of two or more EDF has been developed. Also, the double-pass systems, which are formed to pass the signal twice with the help of reflectors in part of single EDF, have been created. Ultimately, three or more-pass systems has been developed using several EDF and reflectors by increasing the gain of EDFAs [3-21].

In consequence of the rapidly increasing capacity, requires not only high gain but also flat gain characteristics. However, gain spectrum of the EDFA is not flat. This property affects the output signal gain levels and some signal channels lost in ultra-long haul communication systems. For this reason, EDFA gain spectrum must be flattened.

Optical and electronic methods are used to obtain flat gain EDFAs. In electronic methods, high-gain signals are attenuated by the pump laser current that is controlled according to the output gain [22]. On the other hand, in optical methods, gain is flattened completely by using all-optical components [23-30]. Two-stage systems, GFF and FBG are used to provide flat gain spectrums in EDFA [31-37]. In the literature, commonly used techniques are gain flattening/equalization filter (GFF), optical feedback loop, and fibre Bragg grating (FBG).

In a FBG, interlocking effect of propagating modes due

to the change of refractive index occurs between modes passing in opposite directions. Due to the change in refractive index, grating formation is produced in the core of the optical fibre. Under certain conditions known as Bragg condition, reflected light from the grating are added together and a great reflection occurs. Distance of the grating (Λ) is called the grating period. There are four common structures of the refractive index change for FBGs. These are uniform FBG, chirped FBG, tilted FBG, and long period FBG. The grating period is constant in the uniform FBG. The refractive index profile of the grating may be modified to add other features known as a chirp in the chirped FBG. The reflected wavelength changes with the grating period, broadening the reflected spectrum. The change of the refractive index is an angle to the optical axis in a tilted FBG. In long period FBGs, longer periods can be used to achieve much broader responses than a conventional FBG [38]. In FBG, the grating period is less than 1 μm . FBG that operates in reflection mode reflects back from the grating portion of the light that applied to the input of the fibre. This reflectivity reaches to the highest value in the Bragg wavelength. The reflected light spectrum is very narrow and centred at the Bragg wavelength [39]. GFF can be used to eliminate the differences of power of multi-channel signal at the output of the EDFA. Filter contributes to the flattening of the gain spectrum by showing a weakening effect. Generally, a second EDF is used to reduce loss of gain arising from the filter so called two-stage [40].

In the optical feedback loop, the ASE is suppressed by the variable optical attenuator (VOA) and/or circulator and/or faraday rotator mirror. There are several studies in the literature to flat the gain spectrum of EDFAs. Studies in recent years have focused on single and double-pass EDFA, two-stage EDFA and multi-pass EDFA [41-49]. In

the literature, the total gain is flattened by using VOA [23]. Rao et al. suggested to flat the gain spectrum of EDFAs by using long-period fibre grating [24]. Ben-Ezra et al. proposed to use semiconductor optical amplifier (SOA) based on negative feedback loop to adjust the pump power in EDFA [25], H. Zhang et al. analyzed all optical gain clamping EDFA by using fibre loop mirror [26]. Kaler controlled the transitions to add/drop channels in cascaded EDFAs [27]. Lin et al. achieved that decreasing the period and amplitude of power transitions in EDFA with power-shaping technique [28]. Zhao et al. controlled the gain of EDFAs by bending the long period grating [29]. Finally Harun et al. achieved the gain control of double-pass L band EDFA by using ring resonator and two-stage systems [30].

In this study, all optical gain flattening systems for the C and L band EDFAs are analyzed in detail. For this purpose, five configurations are set up and compared. In the second section, the gain and noise spectrum are given and analyzed for each configuration. In the third and fourth sections, the best and the worst configurations, advantages and disadvantages of these configurations are determined.

2. Simulation Setups

In this study, five configurations are set up and simulated in the OptiSystem 12.0 optical software program. These configurations are two-stage EDFA with GFF and FBG, two-stage EDFA with UFBG, single-stage EDFA with FBG, single-stage EDFA with optical loop, and two-stage EDFA with optical feedback loop. The input signal power is -20 dBm for all configurations and input signal wavelengths are 1530-1564 nm for C band and 1570-1610 nm for L band.

In the first study, called as two-stage EDFA with GFF and FBG, gain spectrum of the whole system has been optimized to obtain a flat gain spectrum along the C band. Hence, GFF is placed between two optical fibres and uniform fibre Bragg grating (UFBG) is placed at the end of the second fibre.

Two-stage EDFA with GFF and FBG is shown in Fig. 1. The input signals are applied to fibre isolator that suppresses back reflections via multiple laser source (MLS). Afterwards, input signals and 980 nm pump signal, which has 95 mW powers, are combined in pump coupler. Combined signals are amplified in the first EDF (EDF1) that has 11.5 m and applied GFF that is placed at the end of EDF1. In the second stage, these signals are combined in another pump laser (PL2), which has 95 mW and 980 nm wavelength in a pump coupler. Combined signals are amplified in the second EDF (EDF2) with same length again and applied UFBG that is placed at the end of EDF2. UFBG has 30 nm bandwidths, 50% reflectivity and 1560 nm centre wavelength. These signals are applied to the second fibre isolator (Isolator2) and measured by an optical spectrum analyzer (OSA). EDF lengths and power of the pump lasers are optimized to obtain the minimum

gain fluctuation.

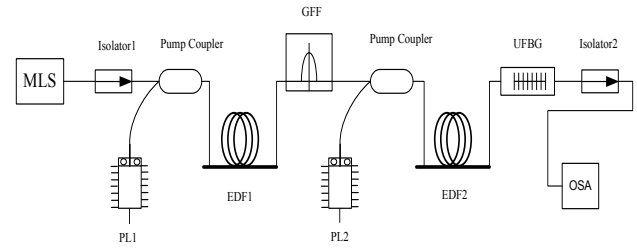


Fig. 1. Two-stage EDFA with GFF and UFBG.

High gain signals between the wavelengths of 1545-1565 nm are attenuated by the GFF of which transmission spectrum is given in Fig. 2 and signal levels are equalized. A part of signal power that has 1550, 1555, 1560, 1565 nm wavelengths is attenuated at a fixed rate by the UFBG that has 30 nm bandwidth, 50% reflectivity and 1560 nm centre wavelength.

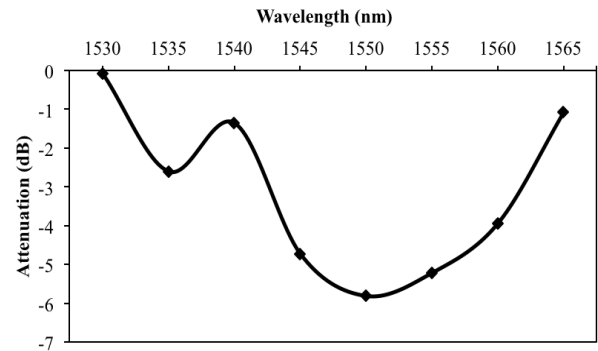


Fig. 2. Transmission spectrum of GFF.

Fig. 3 shows the gain and noise figure spectrum of the proposed two-stage EDFA with GFF and FBG.

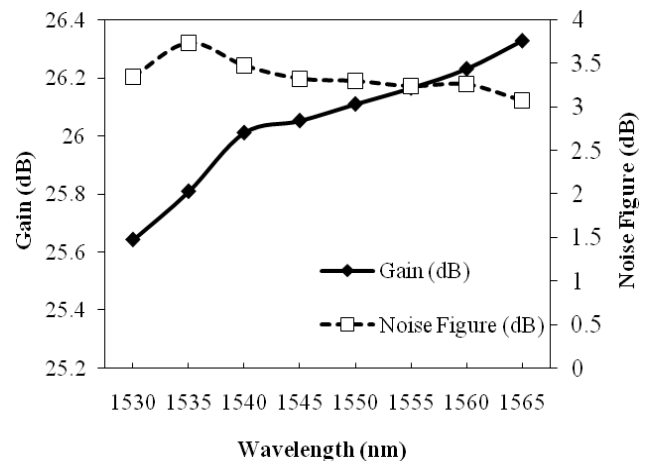


Fig. 3. The gain and noise figure spectrum of the two-stage EDFA with GFF and FBG.

As it can be seen in Fig. 3, the gain spectrum is increased from 1530 to 1565 nm for the proposed system.

The average noise figure is reduced to 3.34 dB with the suppression of ASE. The noise figure is higher at 1535 nm than other wavelengths.

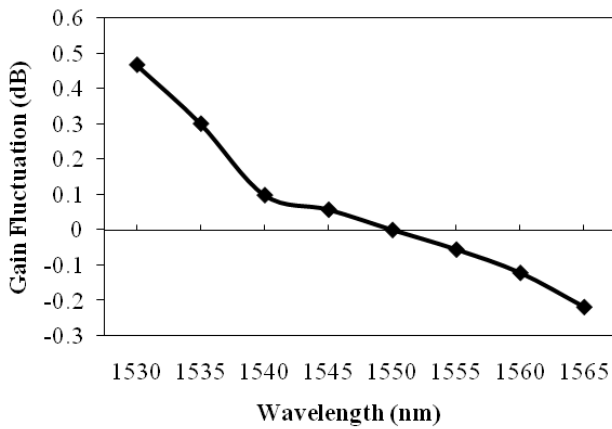


Fig. 4. Normalized gain fluctuation spectrum.

The gain fluctuation spectrum that is normalized for 1550 nm is shown in Fig. 4. In the figure, the gain fluctuation is highly reduced with GFF and UFBG. For the wavelengths between 1530-1565 nm, the gain fluctuations are in the range of -0.2 and 0.5 dB, approximately.

When Fig. 3 and Fig. 4 are analyzed, the gain is increased at 1530, 1535 and 1540 nm wavelength, while it is clipped in the range of 1545-1565 nm and the ripple is reduced to around 0.68 dB. Also, it is observed that better noise figure due to suppressed ASE for each wavelength is obtained between the ranges 1530-1565 nm. In this configuration, it is obtained an approximately 26.04 dB gain and 0.68 dB ripple by using GFF and UFBG in C band two-stage EDFA.

In the second study, called as two-stage EDFA with FBG, gain spectrum of the whole system has been optimized to obtain a flat gain spectrum along the C band. Hence, UFBG1 is placed at the end of the first fibre (EDF1) at the first stage and UFBG2 and FBG are placed at the end of the second fibre (EDF2) in the second stage, respectively.

Two-stage EDFA with FBG is shown in Fig. 5. The input signals are applied to Isolator1 via MLS. Afterwards, input signals and 980 nm pump signal that has 55 mW powers are combined into pump coupler. Combined signals are amplified in first EDF1 (9.5 m) and applied UFBG1 that is placed at the end of the EDF1. FBG acts as an optical reflector at λ_B wavelength. A part of the signal power that has 1550, 1555, 1560 nm wavelength is attenuated at a fixed rate by the UFBG1 that has 25 nm bandwidth, 65% reflectivity and 1555 nm centre wavelength.

In the second stage, signals arising from UFBG1 and 980 nm pump signal that has 55 mW powers are combined in a pump coupler. Combined signals are amplified into EDF2 (10.5 m) again and applied UFBG2, which is placed at the end of the EDF2. A part of the signal power that has

1540, 1545 nm wavelength is attenuated at a fixed rate by the UFBG2 that has 10 nm bandwidth, 40% reflectivity and 1543 nm centre wavelength. The amount of the change in refractive index varies along the length of the period in the FBG that has 1535 nm centre wavelength, 1.45 effective index and 2.7 mm length. A part the signal power, which has 1535 nm wavelength, is reflected with FBG and the final stage of gain flattening is achieved. Then, transmitted signals are applied to Isolator2. These signals are measured by OSA and finally gain and noise spectrum are analyzed. EDF lengths and power of the pump lasers are optimized to obtain the minimum gain fluctuation. During the simulation, UFBG or FBG has been selected according to the reflected power ratio that is constant or variable.

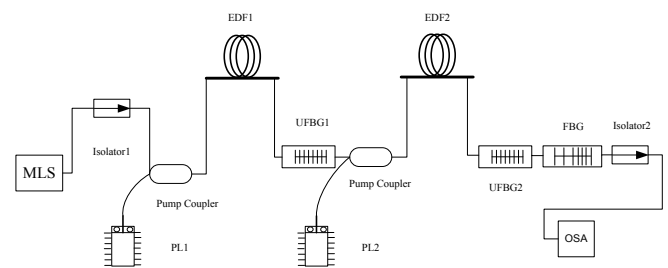


Fig. 5. Two-stage EDFA with FBG.

Fig. 6 shows the gain and noise figure spectrum of the proposed two-stage EDFA with FBG.

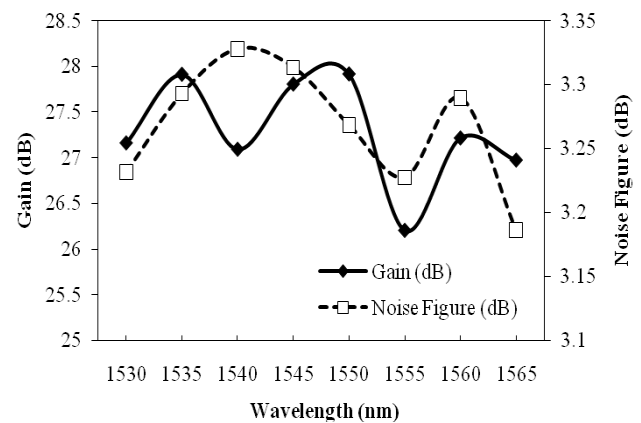


Fig. 6. The gain and noise figure spectrum of the two-stage EDFA with FBG.

Fig. 6 shows the highest gain that is obtained near 1550 nm for the proposed system. The average noise figure is reduced to 3.27 dB with suppression of ASE. The noise figure is the highest at 1540 nm.

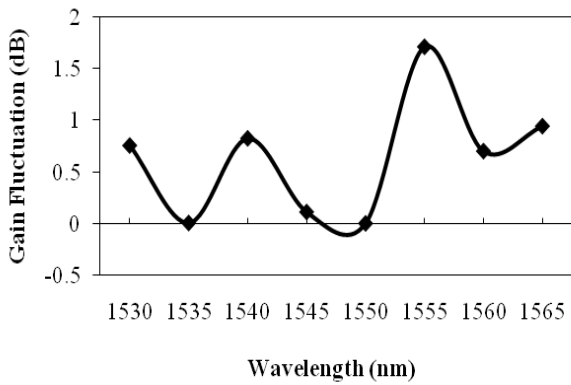


Fig. 7. Normalized gain fluctuation spectrum.

The gain fluctuation spectrum, which is normalized for 1550 nm, is shown in Fig. 7. As it can be seen in Fig. 7, the gain fluctuation is highly reduced by using FBG and UFBG. For the wavelengths between 1530-1565 nm, the gain fluctuations are in the range of 0.004 and 1.71 dB, respectively.

When Fig. 7 is analyzed, the ripple is reduced to about 1.71 dB at the proposed system. Also, it is observed the better noise figure due to suppressed ASE for each wavelength between the ranges of 1530-1565 nm. In this configuration, it is obtained that approximate 27.32 dB gain totally and 1.71 dB ripple using two UFBG and one FBG in C band two-stage EDFA.

In the third study, single-stage EDFA with UFBG, gain spectrum of the whole system has been optimized to obtain a flat gain spectrum along the C band. For this aim, four UFBG are placed at the end of the EDF.

Single-stage EDFA with UFBG is illustrated in Fig. 8. The input signals are applied Isolator via multiple laser source (MLS). Input signals and 980 nm pump signal that has 55 mW powers are combined in pump coupler. Combined signals are amplified in the 16 m EDF and applied UFBG1 that is placed at the end of the EDF. A part of power of signals that has 1550, 1555, 1560 nm wavelength are attenuated at fixed rate by the UFBG1 that has 20 nm bandwidth, 45% reflectivity and 1555 nm centre wavelength.

Signals arisen from UFBG1 are applied UFBG2 that has 10 nm bandwidth, 45% reflectivity and 1547 nm centre wavelength. A part of these signals that has 1545 and 1550 nm wavelengths are reflected at fixed rate by the UFBG2. Then, signals are applied UFBG3 that has 5 nm bandwidth, 30% reflectivity and 1535 nm centre wavelength. A part of these signals that has 1535 nm wavelength is reflected at fixed rate by the UFBG3. Then, signals are applied UFBG4 that has 5 nm bandwidth, 30% reflectivity and 1560 nm centre wavelength. A part of these signals that has 1560 nm wavelength is reflected at fixed rate by the UFBG4. The signals that have 1535, 1545, 1550 and 1560 wavelengths are partially suppressed and the other signals are transmitted. Thus, the gain

fluctuation is minimized along the C band. Transmitted signals are measured by OSA. EDF lengths and power of the pump lasers are optimized to obtain the minimum gain fluctuation.

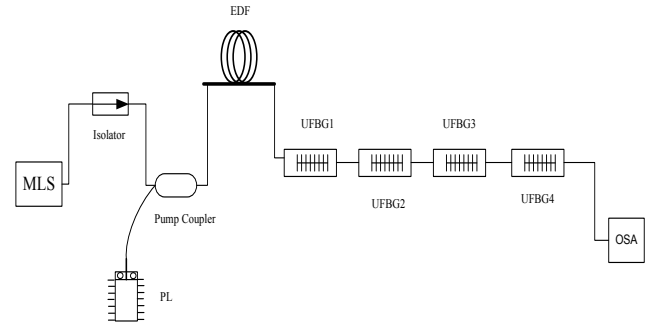


Fig. 8. Single-stage EDFA with UFBG.

Fig. 9 shows the gain and noise figure spectrum of the proposed single-stage EDFA with UFBG.

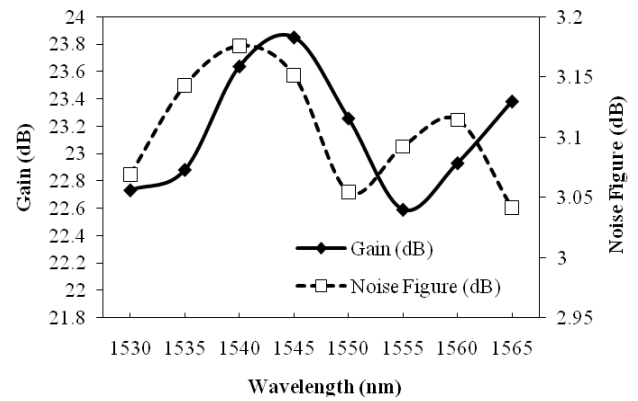


Fig. 9. The gain and noise figure spectrum of the single-stage EDFA with UFBG.

As seen in Fig. 9, the highest gain was obtained near 1545 nm at the proposed system. The average noise figure is reduced 3.11 dB. The noise figure is higher at 1540 nm than other wavelengths.

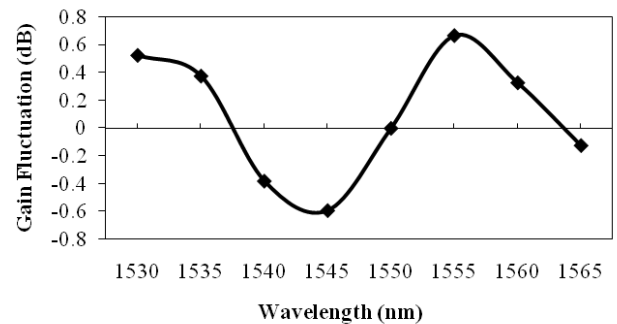


Fig. 10. Normalized gain fluctuation spectrum.

The gain fluctuation spectrum, which is normalized for 1550 nm, is shown in Fig. 10. As it can be seen in Fig. 10, the gain fluctuation is highly reduced by using four UFBG. For between the wavelengths of 1530-1565 nm, the gain fluctuations are in the range of -0.59 and 0.67 dB.

When Fig. 10 is analyzed, the ripple is reduced to 1.26 dB for the proposed system. Also, it is observed that better noise figure is obtained due to suppressed ASE for each wavelengths in the range of 1530-1565 nm. In this configuration, it is obtained an approximate gain of 23.18 dB and 1.26 dB ripple by using four UFBG in C band single-stage EDFA.

In the fourth study, single-stage EDFA with optical loop is used. The gain spectrum of the whole system has been optimized to obtain a flat gain spectrum along the L band. Hence, an optical loop is established using the 17 dB VOA, 2X2 coupler and a circulator to obtain gain flatness.

Single-stage EDFA with optical loop is shown in Fig. 11. The input signals that are generated by MLS and 980 nm pump signal which has 100 mW power which are combined into pump coupler. The combined signals are applied to L band EDF (61 m). Also, the produced signals by the PL2 that has same in PL1 are applied to L band EDF in opposite directions. These signals and ASE reach to a circulator via 2x2 coupler. The signals passes from port 1 towards port 2 of circulator are given into 17 dB VOA. The attenuated signals pass from port 3 towards to port 1 of the circulator. The amplified signals and ASE signals are attenuated and given into the system again by using loop. These signals are passed from Isolator and measured by OSA. EDF lengths and power of the pump lasers are optimized to obtain the minimum gain fluctuation.

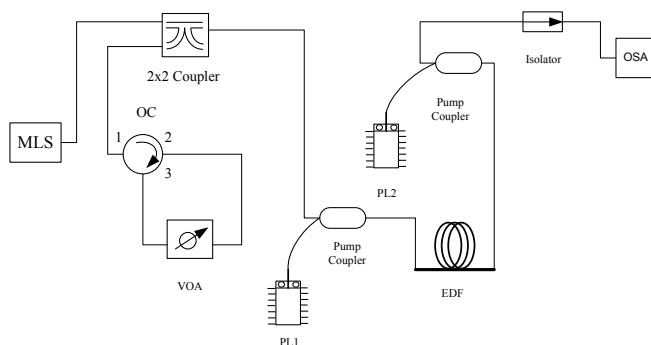


Fig. 11. Single-stage EDFA with optical loop.

Fig. 12 shows gain and noise figure spectrum of the proposed single-stage EDFA with optical loop.

In Fig. 12 highest gain is obtained near 1570 nm for the proposed system. The average noise figure is reduced to 3.52 dB due to the decrement of ASE. The noise figure is higher at 1575 nm than other wavelengths.

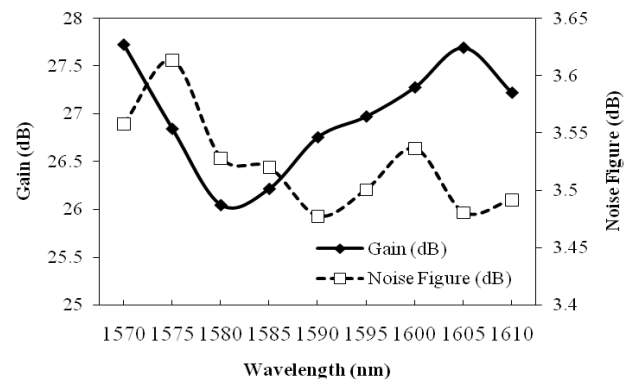


Fig. 12. The gain and noise figure spectrum of the single-stage EDFA with optical loop.

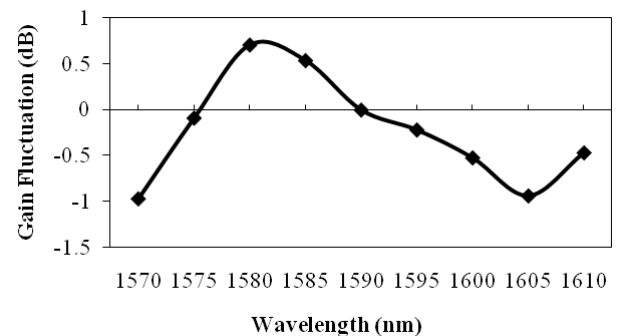


Fig. 13. Normalized gain fluctuation spectrum.

The gain fluctuation spectrum that is normalized for 1590 nm is shown in Fig. 13. An optical loop is established using a circulator, a 2x2 coupler and a VOA at the proposed system and the gain fluctuation is highly reduced. For the wavelengths between 1570-1610 nm, the gain fluctuations are in the range of -0.97 and 0.71 dB. When Fig. 13 is analyzed, the ripple is reduced to 1.68 dB for the proposed system. Also, it is observed that better noise figure is achieved due to the suppressed ASE for each wavelength between the ranges of 1570-1610 nm.

In this configuration, it is obtained that an approximate gain of 27.00 dB is achieved with a 1.68 dB ripple by using an optical loop in single-stage L band EDFA.

In the fifth study, two-stage EDFA with optical feedback loop is used. The gain spectrum of the whole system has been optimized by using two circulators to obtain a flat gain spectrum along the L band.

Two-stage EDFA with optical feedback loop is shown in Fig. 14. The input signals are applied Isolator1 via MLS. After, input signals pass from port 1 towards port 2 of optical circulator (OC1) and these signals and 980 nm pump signal that has 55 mW powers are combined into pump coupler. Combined signals are amplified into EDF1 (33.5 m) and applied Isolator2 that is placed at the end of EDF1. These signals and 1480 nm pump signal that have

107.9 mW powers are combined into pump coupler and combined signals are amplified into EDF2 (100 m) again and applied Isolator3 after passing from port 1 towards port 2 of OC2. Thus, the transmitted signals are measured by the OSA and gain and noise figure of the signals are analyzed. Third port of the circulators which are used in the system are connected each other. In this way, the ASE that consists in EDF1 is amplified in EDF2 again and delivered to the output at the direction of transmitted signals. EDF lengths and power of the pump lasers are optimized to obtain the minimum gain fluctuation.

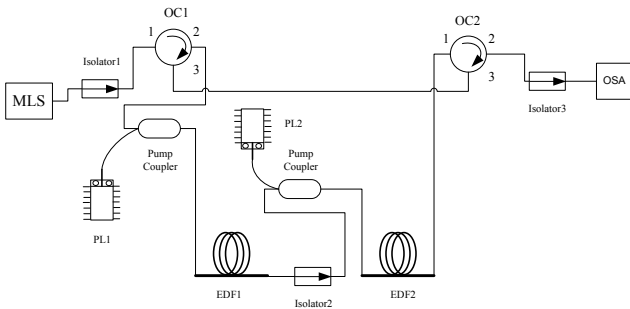


Fig. 14. Two-stage EDFA with optical feedback loop

Fig. 15 shows the gain and noise figure spectrum of the proposed two-stage EDFA with optical feedback loop.

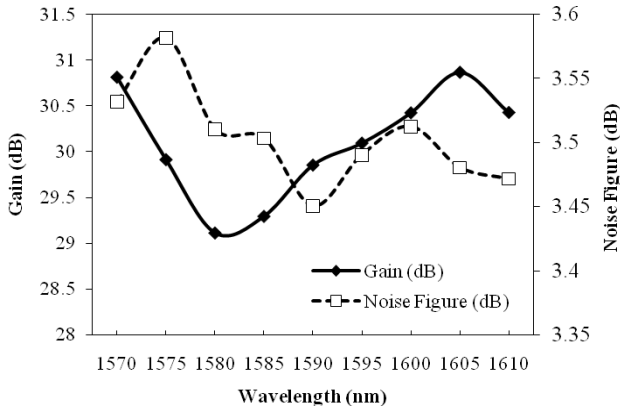


Fig. 15. The gain and noise figure spectrum of the two-stage EDFA with optical feedback loop.

It can be observed in Fig. 15 that the highest gain is obtained near 1605 nm for the proposed system. The average noise figure is reduced to 3.50 dB with the decrease in ASE. The noise figure is highest at 1575 nm.

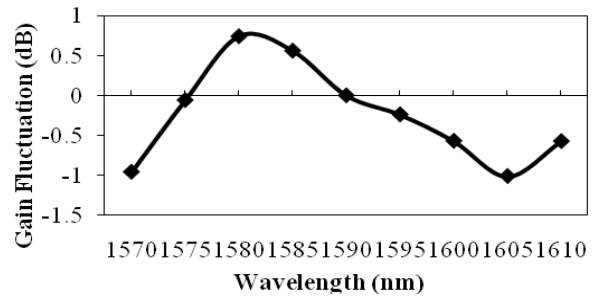


Fig. 16. Normalized gain fluctuation spectrum.

The gain fluctuation spectrum that is normalized for 1590 nm is shown in Fig. 16. The gain fluctuation is highly reduced by using two circulators. For the wavelengths between 1570-1610 nm, the gain fluctuations are in the range of -1.01 and 0.74 dB.

When Fig. 16 is analyzed, the ripple is reduced to 1.75 dB for the proposed configuration. Also, it is observed better noise figure due to suppressed ASE for each wavelength range between 1570 and 1610 nm.

In this configuration, it is obtained a 30.13 dB gain and 1.75 dB ripple by using two circulators with same port 3 connections

3. Results and discussions

In this study, five configurations are set up and each configuration is analyzed in detail. The gain and noise spectrum is given for each configuration and the effects of using components on gain, noise and ripple are analyzed. The best and worst configurations are determined in terms of gain, noise and ripple. Table 1. shows the results of all simulations.

Table 1. The results of the simulations for all configurations.

| Configuration | Band | Gain (dB) | Noise (dB) | Ripple (dB) | Normalised Cost |
|--|--------------|-----------|------------|-------------|-----------------|
| 1. Two-stage EDFA with GFF and UFBG | 1530-1565 nm | 26.04 | 3.34 | 0.68 | 12 |
| 2. Two-stage EDFA with FBG | 1530-1565 nm | 27.32 | 3.27 | 1.71 | 13 |
| 3. Single-stage EDFA with UFBG | 1530-1565 nm | 23.18 | 3.11 | 1.26 | 10 |
| 4. Single-stage EDFA with optical loop | 1570-1610 nm | 27.00 | 3.52 | 1.68 | 11 |
| 5. Two-stage EDFA with optical feedback loop | 1570-1610 nm | 30.13 | 3.50 | 1.75 | 13 |

When Table 1. is analyzed, the highest gain is obtained by using two circulators in two-stage L band EDFA. On the other hand, the lowest gain is obtained with using four UFBG in single-stage C band EDFA. While the highest gain is obtained in the fifth configuration, the lowest ripple is obtained in the first configuration. The worst ripple is obtained in fifth configuration. The noise figures of fourth and fifth configurations are near to each other and higher than other configurations. The best noise figure is obtained by using the third configuration.

4. Conclusions

In this study, three C and two L band EDFA configurations are considered to obtain better gain flatness characteristics. When the results of the simulations are compared, it can be observed that the two-stage systems has better in gain around 30.13 dB for L band and two-stage EDFA with FBG has the best gain around 27.32 dB for C band. However, the least gain variation is obtained only 0.68 dB at the two-stage EDFA with GFF and FBG for C band. In addition, almost the same gain variations are obtained in both configurations for L band. As a conclusion, the designers should select the best configuration that has the best price, and the simplest design.

References

- [1] M. Yamada, NTT Technical Review, **2**(12), 34 (2004).
- [2] T. Sakamoto, A. Mori, H. Masuda, H. Ono, NTT Technical Review, **2**(12), 38 (2004).
- [3] B. Bouzid, M. K. Abdullah, M. A. Mahdi, Laser Physics, **18**(4), 460 (2008).
- [4] T. C. Liang, S. Hsu, Optics Comm., **281**(5), 1134 (2008).
- [5] M. Z. Jamaludin, M. K. Abdullah, F. Abdullah, A. F. Abas, M. A. Mahdi, F. Rahman, Optics and Laser Technol., **40**(2), 270 (2008).
- [6] A. W. Naji, M. S. Z. Abidin, M. H. Al-Mansoori, A. R. Faidz, M. A. Mahdi, Laser Physics Lett., **4**(2), 145 (2007).
- [7] C. L. Chang, L. Wang and Y. J. Chiang, Optics Comm., **267**(1), 108 (2006).
- [8] A. Altuncu, IEEE Photon. Technol. Lett., **18**(9), 1043 (2006).
- [9] S. W. Harun, N. M. Samsuri H. Ahmad, Pramana-Journal of Physics, **66**(3), 539 (2006).
- [10] L. L. Yi, L. Zhan, W. S. Hu, Y. X. Xia, Optics Express, **14**(2), 570 (2006).
- [11] L. L. Yi, L. Zhan, C. S. Taung, S. Y. Luo, W. S. Hu, Y. K. Su, Y. X. Xia, L. F. Leng, Optics Express, **13**(12), 4519 (2005).
- [12] J. H. Ji, L. Zhan, L. L. Yi, C. C. Tang, Q. H. Ye, Y. X. Xia, J. of Lightwave Technol., **23**(3), 1375 (2005).
- [13] N. M. Samsuri, S. W. Harun and H. Ahmad, Laser Physics Lett., **1**(12), 610 (2004).
- [14] S. W. Harun, N. M. Samsuri and H. Ahmad, Laser Physics Lett., **2**(1), 36-38 (2005).
- [15] S. W. Harun, N. M. Samsuri, H. Ahmad Microwave and Optical Technol. Lett., **43**(6), 484 (2004).
- [16] A. W. Naji, M. S. Z. Abidin, A. M. Kassir, M. H. Al-Mansoori, M. K. Abdullah, M. A. Mahdi, Microwave and Optical Technol. Lett., **43**(1), 38 (2004).
- [17] L. L. Yi, L. Zhan, J. H. Ji, Q. H. Ye, Y. X. Xia, IEEE Photon. Technol. Lett., **16**(4), 1005 (2004).
- [18] S. W. Harun, H. Ahmad, Microwave and Optical Technol. Lett., **40**(2), 112 (2004).
- [19] S. W. Harun, P. Poopalan and H. Ahmad, Indian Journal of Physics, **77B**(4), 435 (2003).
- [20] S. W. Harun, P. Poopalan and H. Ahmad, IEEE Photon. Technol. Lett., **14**(3), 296 (2002).
- [21] S. W. Harun, H. Ahmad, Chinese Physics Lett., **21**(10), 1954 (2004).
- [22] M. Yucel, Microwave and Optical Technology Letters, **53**(11), 2703 (2011).
- [23] X. Feng, T. Jin, Y. Wang, Q. Wang, X. Liu, J. Peng, Optics Communications, **213**(4-6), 285 (2002).
- [24] Y. J. Rao, A. Z. Hu and Y. C. Niu, Optics Communications, **244**(1-6), 137 (2005).
- [25] Y. Ben-Ezra, M. Haridim and B. I. Lembrikov, IEEE Journal of Quantum Electronics, **42**(11-12), 1209 (2006).
- [26] H. Zhang, Q. Y. Dou, Y. Jin, T. Guo, L. Liu, Y. Liu, S. Yuan, X. Dong, Microwave and Optical Technology Letters, **48**(5), 852 (2006).
- [27] R. S. Kaler, Optik, **122**(5), 444 (2011).
- [28] W. Lin, R. S. Wolff and B. Mumei, Optical Switching and Networking, **5**(4), 188 (2008).
- [29] C. L. Zhao, H. Y. Tam, B. O. Guan, X. Dong, P. K. A. Wai, Optics Communications, **225**(1-3), 157 (2003).
- [30] S. W. Harun, N. M. Samsuri, R. Poopalan, H. Ahmad, Optik, **115**(11), 525 (2004).
- [31] M. Yucel, H. H. Goktas, J. Fac. Eng. Archit. Gazi Univ., **22**, 863 (2007).
- [32] G. Yenilmez, M. Yucel, IEEE 22th Signal Process. and Comm. Appl. Conf. SIU, 2014, Trabzon, Turkey.
- [33] H. H. Goktas, M. Yucel, J. Inst. Sci. Technol. Sakarya Univ., **10**, 10 (2006).
- [34] S. Dung, J. C. Chi and S. Wen, Electronics Letters, **34**(6), 555 (1998).
- [35] H. B. Choi, J. M. Oh, D. Lee, S. J. Ahn, B. S. Park, S. B. Lee, Optics Comm., **213**, 63 (2002).
- [36] M. A. Mahdi, S. J. Sheih, Optics Comm., **234**, 229 (2004).
- [37] K. Mizuno, Y. Nishi, Y. Mimura, Y. Lida, H. Matsuura, D. Yoon, O. Aso, T. Yamamoto, T. Toratani, Y. Ono, A. Yo, Furukawa Review, **19**, 53 (2000).
- [38] J. Canning, M. G. Sceats, Electron. Lett., **30**(16), 1344 (1994).
- [39] L. Karaman, N. Ö. Ünverdi, M.Sc. Thesis, Yıldız Technical University, 2009.

- [40] H. H. Goktas, M. Yucel, Sakarya Univ. Journal of Sci., **10**(1), 10 (2006).
- [41] M. Yucel, H. H. Goktas and G. Akkaya, M. Yucel, H. H. Goktas, IEEE 15th Signal Process. and Comm. Appl. Conf. SIU, 2012, Fethiye, Turkey.
- [42] M. Yucel, H. H. Goktas, IEEE 15th Signal Process. and Comm. Appl. Conf. SIU, 2007, Eskisehir, Turkey
- [43] M. Yucel, Z. Aslan, Microwave and Optical Technology Letters, **55**(11), 2525 (2013).
- [44] M. Yucel, H. H. Goktas, J. Fac. Eng. Archit. Gazi Univ., **27**(2), 237 (2012).
- [45] M. Yucel, H. H. Goktas, Journal of Applied Sciences, **8**(23), 4464 (2008).
- [46] M. Yucel, H. H. Goktas and O. Ozkaraca, J. Fac. Eng. Arch. Gazi Univ., **25**(3), 635 (2010).
- [47] M. Yucel, H. H. Goktas and F. V. Celebi, IEEE 19th Signal Process. and Comm. Appl. Conf. SIU, 2011, Kemer, Turkey.
- [48] M. Yucel, F. V. Celebi and H. H. Goktas, Optik - Int. J. Light Electron Opt., **122**(10), 872 (2011).
- [49] M. Yucel, H. H. Goktas, IEEE 16th Signal Process. and Comm. Appl. Conf. SIU, 2008, Didim, Turkey.

*Corresponding author: muyucel@gazi.edu.tr